J. Fluid Mech. (1980), *vol.* 98, *part* 4, *pp.* 803–818
Printed in Great Britain

Shelves and the Korteweg–de Vries equation

By C. J. KNICKERBOCKER AND ALAN C. NEWELL

Department of Mathematics and Computer Science, Clarkson College, Potsdam, NY 13676

(Received 14 November 1978 and in revised form 1 October 1979)

An extension of the analytical results of Kaup & Newell (1978) concerning the effect of a perturbation on a solitary wave of the Korteweg–de Vries equation is given and numerical studies are conducted to verify the conclusions. In all cases, the numerical results agree with the results predicted by the theory. The most striking feature of the perturbed flow is the presence of a shelf in the lee of the solitary wave whose role is to absorb (provide) the extra mass which is created (depleted) by the perturbation.

1. Introduction and discussion

The problem of the propagation of a shallow-water solitary wave in a canal of slowly varying depth has been the subject of several papers in the recent literature. Although the changing depth causes reflexions (Peregrine 1967; Miles 1979); to a good approximation the unidirectional propagation is well described by the perturbed Korteweg–de Vries equation (PKdV) (Johnson 1973*a*; Kakutani 1971),

$$q_t + 6qq_x + q_{xxx} = -\Gamma(t)\,q, \quad 0 < \Gamma \ll 1. \tag{1.1}$$

In the context of water waves, the local depth is $hD(\epsilon^{\frac{3}{2}}X/h) + \epsilon hN(\epsilon^{\frac{1}{2}}X/h,\ \epsilon^{\frac{1}{2}}g^{\frac{1}{2}}h^{-\frac{1}{2}}T)$ with X and T the dimensional space and time co-ordinates respectively; the co-ordinate x is the local retarded time

$$x = \frac{1}{\epsilon}\int_0^{\epsilon^{\frac{1}{2}}X/h} \frac{ds}{D^{\frac{1}{2}}(s)} - \frac{(gh\epsilon)^{\frac{1}{2}}}{h}T; \quad t = \frac{1}{6}\int_0^{\epsilon^{\frac{1}{2}}X/h} D^{\frac{1}{2}}(s)\,ds$$

is a measure of the distance along the channel from the point where the depth begins to change. The right-going component of the disturbed elevation N is given by $\frac{2}{3}D^2q(x,t)$ and $\Gamma(t)$ is $9D_t/4D$ which is assumed small; namely D changes slowly with respect to the length scale of the disturbance.

It is natural to exploit the smallness of $\Gamma(t)$ and to write as a first approximation the solution to (1.1) in terms of the solution of the unperturbed problem allowing those quantities which are constants of the latter to vary slowly in time. Ott & Sudan (1970), assuming that the basic solution has the form of a soliton

$$q(x,t) = 2\eta^2 \operatorname{sech}^2 \eta(x-\bar{x}), \quad \bar{x}_t = 4\eta^2 \tag{1.2}$$

and using the conservation law (energy)

$$\frac{\partial}{\partial t}\int_{-\infty}^{\infty} q^2\,dx = -2\Gamma(t)\int_{-\infty}^{\infty} q^2\,dx, \tag{1.3}$$

0022-1120/80/4463-1790 $02.00

found that $\eta(t)$ satisfies $$\eta_t = -\tfrac{2}{3}\Gamma\eta, \tag{1.4}$$

which we shall see is a correct result. They did not explain, however, the fact that neither of the expressions for conservation of mass (here we speak of conservation of mass in the sense of the KdV equation; in the water wave context some of the actual mass is reflected),

$$\frac{\partial}{\partial t}\int_{-\infty}^{\infty} q\,dx = -\Gamma(t)\int_{-\infty}^{\infty} q\,dx, \tag{1.5}$$

nor of first moment

$$\frac{\partial}{\partial t}\int_{-\infty}^{\infty} xq\,dx = 3\int_{-\infty}^{\infty} q^2\,dx - \Gamma(t)\int_{-\infty}^{\infty} xq\,dx, \tag{1.6}$$

are satisfied to leading order. Each of the relations (1.3), (1.5), (1.6) may be integrated exactly (Leibovich & Randall 1971),

$$M(t) = \int_{-\infty}^{\infty} q\,dx = M(t_0)\exp\left(-\int_{t_0}^{t}\Gamma(s)\,ds\right), \tag{1.7a}$$

$$E(t) = \int_{-\infty}^{\infty} q^2\,dx = E(t_0)\exp\left(-2\int_{t_0}^{t}\Gamma(s)\,ds\right) \tag{1.7b}$$

and

$$G(t) = \int_{-\infty}^{\infty} xq\,dx = \left[G(t_0) + 3E(t_0)\int_{t_0}^{t} ds\exp\left(-\int_{t_0}^{s}\Gamma(r)\,dr\right)\right]\exp\left(-\int_{t_0}^{t}\Gamma(s)\,ds\right). \tag{1.7c}$$

Several authors (Grimshaw 1970, 1971; Johnson 1973*b*; Leibovich & Randall 1973) have examined the propagation of a solitary wave over an uneven bottom topography in some detail. Johnson (1973*b*) and Leibovich & Randall (1973) work with (1.1) directly and attempt to find an asymptotic representation of the solution in the form

$$q(x,t) = q_0(x,t) + \sigma q_1(x,t) + \ldots, \tag{1.8}$$

where σ, $0 < \epsilon \ll \sigma \ll 1$, is a measure of the amplitude of $\Gamma(t)$ and $q_0(x,t)$, the leading approximation, is given by (1.2). By demanding that the asymptotic series (1.8) remains a uniformly valid description of the solution $q(x,t)$ over long time (σ^{-1}), they found that $\eta(t)$ obeys (1.4). However, they were unable to find a solution $q_1(x,t)$ which tends to zero both as $x\to\infty$ and $x\to-\infty$. In fact, they found that, as $x\to-\infty$, $q_1\to\Gamma/3\eta\sigma$, which renders (1.8) non-uniform and seems to indicate that the mass

$$\int_{-\infty}^{\infty} q\,dx$$

is infinite. Clearly there is something non-uniform about the expansion (1.8), a point to which we will return. Nevertheless, as we shall see, the results are almost correct and indeed a shelf does form behind the solitary wave. However, it has a finite range, a fact observed numerically by Leibovich & Randall (1973) but not explained theoretically.

The dilemma of infinite mass and the role of the shelf was first explained by Kaup & Newell (1978) (hereinafter referred to as KN) who used a totally different method (also used by Karpman & Maslov (1977); we should also mention that some of these results were obtained by Ko & Kuehl (1978) by a direct method after they were familiar with the results of Kaup & Newell). They exploited the fact that the unper-

turbed equation (1.1) is exactly integrable. By exactly integrable, we mean the following. The KdV equation is an infinite-dimensional Hamiltonian system (Gardner 1971; Zakharov & Faddeev 1971; Flaschka & Newell 1975) which may be written

$$q_t = \frac{\partial}{\partial x}\frac{\delta H}{\delta q}, \quad H = \frac{1}{2}\int_{-\infty}^{\infty}(q_x^2 - 2q^3)\,dx \tag{1.9}$$

and $\delta/\delta q$ is the variational derivative. The inverse scattering transform (Gardner *et al.* 1967, 1974), is a canonical transformation (preserves the form of Hamilton's equations) which carries the old co-ordinates $q(x,t)$, $-\infty < x < \infty$, to new ones which are defined by the scattering data S,

$$S = \{(\gamma_k, \zeta_k = i\eta_k)|_{k=1}^{N}, R(\zeta), \zeta \text{ real}\} \tag{1.10a}$$

of the eigenvalue problem

$$\psi_{xx} + (\zeta^2 + q(x,t))\,\psi = 0, \quad -\infty < x < \infty. \tag{1.10b}$$

In S, the quantities η_k are the bound-state eigenvalues, the γ_k are the normalization constants for the corresponding eigenfunctions and $R(\zeta)$ is the reflexion coefficient. If $q(x,t)$ evolves according to the KdV equation (or any member of the KdV family), then the functions $-2\eta_k^2$ and $(-2\zeta/\pi)\ln(1-|R|^2)$ are action variables and therefore constants of the motion; their angle counterparts, which change linearly in time, are proportional to $\ln\gamma_k$ and $\arg R(\zeta)$ respectively, and the Hamiltonian H in the new co-ordinates is an additive function of the action variables. Each η_k gives rise to a soliton which when physically separated from the other solution components has the form $2\eta_k^2\,\mathrm{sech}^2\,\eta_k(x-\bar{x}_k)$ with $\bar{x}_{kt} = 4\eta_k^2$, where $\gamma_k = 2i\eta_k \exp[2\eta_k \bar{x}_k]$. Thus the action variable η prescribes the constant amplitude, shape and speed of the soliton; the angle variable γ or $\bar{x}$ defines its position. The function $R(\zeta)$, the reflexion coefficient, measures the degree to which the continuous spectrum is excited. For a pure soliton state or reflexionless potential $q(x,t)$, $R(\zeta) \equiv 0$. In general, however, $q(x,t)$ is expressed as a series in terms of the squared eigenfunctions of (1.10*b*), wherein contributions from both the continuous and discrete spectra are included,

$$q(x,t) = \frac{2}{i\pi}\int_{-\infty}^{\infty}\zeta R(\zeta)\,\psi^2(x,t,\zeta)\,d\zeta - 4\sum_{1}^{N}\gamma_k\,\zeta_k\,\psi_k^2(x,t,\zeta_k). \tag{1.11}$$

The solution component corresponding to the continuous spectrum gives rise to that portion of the solution which is oscillatory and dispersive in nature. We can therefore think of the KdV equation as being separated into its various normal modes (ψ^2, ψ_k^2) by the inverse scattering transform.

The effect of a perturbation is to render (1.1) no longer exactly separable. Instead the normal modes can become mixed; an initial state consisting only of solitons can stimulate radiation and in certain cases vice versa. If the perturbation term is small, then it is natural to treat the system by writing down the equations for the rates of change of the action variables and allowing the leading-order approximations of the latter to vary slowly so as to suppress any non-uniformities appearing in the perturbation expansions for these quantities. This is the method used by KN to analyse the effects of various typical perturbations on the canonical equations of inverse scattering theory and is a natural generalization of classical perturbation methods for finite-dimensional Hamiltonian systems.

The principal new result of the KN approach is the resolution of the infinite mass dilemma. What happens is that the continuous spectrum is excited by a resonance due to the interaction between the soliton and the perturbation. The quantity $\zeta R(\zeta)$ develops a Dirac delta-function behaviour at $\zeta = 0$. The corresponding structure in physical space is a shelf of almost constant height which stretches between the position ($x = 0$) of the soliton when the perturbation was just switched on and the solitary wave's present position. In the original co-ordinate frame, the shelf stretches from the soliton to the position to which an infinitesimal disturbance would have travelled from the point where the topography first changed. As the solitary wave moves, new shelf (if $\Gamma > 0$, it is a shelf of depression, if $\Gamma < 0$ of elevation) is continuously formed and the extra mass depleted or created is exactly the amount needed to satisfy (1.7*a*) and (1.7*c*). Although it was not originally noted by KN, the amplitude of the shelf continues to evolve after its initial formation due to the influence of the perturbation, a point observed by the present authors (Newell 1978) and independently by Miles (1979). The transition between the shelf and the $q = 0$ state at $x = 0$ is achieved through a series of decaying oscillations (the integral of an Airy function).

Before we give the analytical and numerical results in the next two sections, we make the following remarks. The first concerns the connexion between the KN approach and the straightforward method of perturbing (1.1) directly to obtain

$$q_{0t} + 6q_0 q_{0x} + q_{0xxx} = 0, \tag{1.12a}$$

$$q_{1t} + 6q_0 q_{1x} + 6q_1 q_{0x} + q_{1xxx} = -(1/\sigma)\,\Gamma(t)\, q_0, \tag{1.12b}$$

and so on. The question now arises as to how to solve (1.12*b*). If $q_0(x,t)$ is a solitary wave with phase $\theta = x - \int 4\eta^2\, dt$ and if one asks, as Johnson and Leibovich & Randall did, for solutions $q_1(x,t)$ which depend on the fast scale x and t only through the combination θ and a slow scale σx or σt, then (1.12*b*) is an ordinary differential equation whose solution has the property that $q_1 \to \Gamma/3\eta\sigma$ as x and $\theta \to -\infty$. In other words, if one simplifies (1.12*b*) by making the ansatz $q = q(\theta, \sigma x \text{ or } \sigma t)$, one looks at the problem from the frame of reference of the solitary wave, from which vantage point the shelf looks infinite, and one therefore loses information about the initial onset of the perturbation. Thus the ansatz $q = q(\theta, \sigma x \text{ or } \sigma t)$ fails because, although the shelf amplitude is slowly varying, its range is not. It also fails at the point where q_1 must make the reverse transition from $-\Gamma/3\eta\sigma$ to zero. Near that point, and indeed away from the solitary wave, q_0 is asymptotically zero and q_1 satisfies $q_{1t} + q_{1xxx} = 0$, which together with the local boundary conditions $q_1(x \to -\infty, t) = 0$, $q_1(x \to +\infty, t) = -\Gamma/3\eta\sigma$ is satisfied by the integral of an Airy function, in fact, exactly (2.5). However as we shall see in §§ 2 and 3, for long times, account must be taken of the further evolution of the shelf after its initial creation; this will mean in fact that the second boundary condition on $q_1(x,t)$ will be $q_1(x \to \infty, t) = -(\Gamma/3\eta(0)\,\sigma) \exp\left(-\int_0^t \Gamma(s)\, ds\right)$. One can calculate the position at which the reverse transition must occur by using the exact mass-balance equation (1.7*a*).

There is no doubt, then, that a direct perturbation can be successful, provided one understands *a priori* the nature of the solution. The important thing to check is whether the slow change of the soliton parameter (or parameters) can simultaneously satisfy all the conservation relations; in general, it will not. When it does not, the

solution will no longer be adiabatic; i.e. a slowly varying solitary wave. Nevertheless, as we have seen, using a judicious combination of the perturbation equations and the conservation laws one can obtain the solution by direct methods. Indeed this is the only approach available if the problem is not exactly integrable in the first approximation. However, when it is, we emphasize that all these results appear quite naturally when one takes advantage of the exact integrability of the leading-order equation and inverse scattering theory.

Furthermore, if $q_0(x,t)$ is not simply a soliton but a more complicated solution of (1.12*a*), then it is extremely difficult to find, by direct means, the appropriate basis for which the left-hand side of (1.12*b*), which is then a partial differential equation, separates. The answer is provided by inverse-scattering theory (Newell 1980), which tells us that the correct basis for expanding $q_1(x,t)$ is

$$E = \left\{\frac{\partial\phi^2}{\partial x}(x,\zeta),\ \zeta\,\text{real};\ \left(\frac{\partial\phi_k^2}{\partial x},\ \frac{\partial^2\phi_k^2}{\partial x\,\partial\zeta}\right)_1^N\right\},$$

which is adjoint to the set $F = \{\psi^2(x,\zeta),\ \zeta\,\text{real};\ (\psi_k^2,\ \partial\psi_k^2/\partial\zeta)_1^N\}$, where $\phi(x,\zeta)$ ($\psi(x,\zeta)$) is the solution of (1.10*b*) which behaves as $e^{-i\zeta x}$ ($e^{i\zeta x}$) as $x\to-\infty$ ($+\infty$). Indeed multiplying (1.12*b*) by $\psi^2(x,\zeta,t)$, integrating over $(-\infty,\infty)$ in x, using the expression

$$\psi_t = (q_{0x} - 4i\zeta^3)\,\psi + (4\zeta^2 - 2q_0)\,\psi_x,$$

for the time dependence of ψ, gives us exactly the expressions we would have obtained by the KN approach. Thus in order to separate the perturbed system, we are led back to the same expressions for the perturbed action-angle variables as we would have obtained using the KN method.

Our second remark emphasizes the point that in the KN method no *a priori* ansatz is made concerning the solution structure. All we do is give the initial values of the action and angle variables (e.g. the amplitude and position of the soliton before the perturbation is switched on). Then, no matter how $q(x,t)$ evolves, the scattering data S, see (1.10*a*), is always uniquely defined, the eigenfunctions $\psi(x,t,\zeta)$ always computable in principle and $q(x,t)$ may be written down through (1.11). We stress that the structure of the kth soliton is given by $q = -4\gamma_k\,\zeta_k\,\psi_k^2$. The initial shape is

$$q = 2\eta_k^2\,\mathrm{sech}^2\,\eta_k(x-\bar{x}_k)$$

but one is not guaranteed that the soliton shape is always given by the hyperbolic secant. In the present case, the long-time behaviour of the solitary wave structure can be written as $2\eta_k^2\,\mathrm{sech}^2\,\eta_k(x-\tilde{x}_k)$ except that now $\tilde{x}_k$ is a modification of $\bar{x}_k$, the original angle variable.

Finally we mention that the height of the reflected shelf has been calculated by Miles (1979).

2. Analytical results

For $t < 0$, a soliton (1.2) with $\eta = \eta_0$ travels unperturbed. At $t = 0$, the soliton arrives at $x = 0$ and the perturbation is switched on. Our goal is to monitor the subsequent evolution of $q(x,t)$ to leading order. It is stressed that even though the shelf has amplitude of order Γ, over long time it makes an order one contribution to both the

mass and first moment balance. By examining the change in the scattering data, KN found to leading order that

$$\eta_t = -\tfrac{2}{3}\Gamma\eta, \tag{2.1a}$$

$$\tilde{x}_t = 4\eta^2 + O(\Gamma), \tag{2.1b}$$

where $\tilde{x}$ is a measure of the position of the solitary wave (e.g. the position of its maximum).

As already mentioned, the interaction of the soliton with the perturbation give rise to a resonance which leads to a non-decaying component of the solution connected with the continuous spectrum. Indeed for order one times, KN found that this contribution (calculated by using (1.11)) is given by

$$q_c(x,t) = \frac{\Gamma}{6\pi\eta}\tanh^2\eta(x-\tilde{x})\int_{-\infty}^{\infty}\frac{\sin 2\zeta(x-\tilde{x}) - \sin 2\zeta(x+4\zeta^2 t)}{2\zeta}d(2\zeta) \tag{2.2}$$

$$= \frac{\Gamma}{6\pi\eta}\tanh^2\eta(x-\tilde{x})\left[\pi\,\mathrm{sgn}\,(x-\tilde{x}) - \frac{\pi}{3} - 2\pi\int_0^{x/(3t)^{\frac{1}{3}}}\mathrm{Ai}(s)\,ds\right], \tag{2.3}$$

where $\mathrm{sgn}\,(x) = 1$ for $x \geqslant 0$, $\mathrm{sgn}\,(x) = -1$ for $x < 0$. For $x > \tilde{x} > 0$, the term in the brackets is zero. For $0 < x < \tilde{x}$ (and for those x where $\tanh^2\eta(x-\tilde{x}) \simeq 1$),

$$q_c(x,t) \sim -\frac{\Gamma}{3\eta} + \frac{\Gamma}{6\pi^{\frac{1}{2}}\eta}\left(\frac{x}{(3t)^{\frac{1}{3}}}\right)^{-\frac{3}{4}}\exp\left(-\frac{2}{3}\left(\frac{x}{(3t)^{\frac{1}{3}}}\right)^{\frac{3}{2}}\right); \tag{2.4}$$

for $x < 0$,

$$q_c(x,t) \sim -\frac{\Gamma}{3\pi^{\frac{1}{2}}\eta}\left(\frac{-x}{(3t)^{\frac{1}{3}}}\right)^{-\frac{3}{4}}\cos\left(\frac{2}{3}\left(\frac{-x}{(3t)^{\frac{1}{3}}}\right)^{\frac{3}{2}} + \frac{\pi}{4}\right). \tag{2.5}$$

Thus between $x = 0$ and $x = \tilde{x}$, the position of the solitary wave, a shelf of height $-\Gamma/3\eta$ is created. At both $x = 0$ and $x = \tilde{x}$ the transitions to the respective solitary wave and zero states are smooth. KN pointed out how this shelf accounts for the *rate* of the extra mass created ($\Gamma < 0$; depth-decreasing case) per unit distance, mass which is not absorbed by the amplifying soliton:

$$\frac{\partial}{\partial t}\int_{-\infty}^{\infty} q\,dx = \frac{\partial}{\partial t}\int_{-\infty}^{\infty} q_s\,dx + \frac{\partial}{\partial t}\int_0^{\tilde{x}} q_c\,dx = 4\eta_t + q_c(\tilde{x})\,\tilde{x}_t$$

$$= -\tfrac{2}{3}\Gamma(4\eta) - \tfrac{1}{3}\Gamma(4\eta) = -\Gamma(4\eta),$$

the exact result. However as pointed out by the authors (Newell 1978; this point has also been noted by Miles 1979) the calculation of shelf height for times $1/\Gamma$ is only valid immediately behind the solitary wave. The subsequent evolution of the shelf is most easily calculated from (1.1) directly; the nonlinear and dispersion terms are negligible. Then at $\tilde{t}$ when the solitary wave is at $\tilde{x}(\tilde{t}) = \int_0^{\tilde{t}} 4\eta^2\,dt$, the height of the shelf $q_c(x,\tilde{t})$ at the point x is

$$q(x,\tilde{t}) = \frac{-\Gamma}{3\eta(\tilde{t})}\exp\left(\int_{\tilde{t}}^{t(x)}\Gamma(s)\,ds\right), \quad 0 < x < \tilde{x}, \tag{2.6}$$

$$= 0 \quad \text{otherwise},$$

where $t = t(x)$ through the integration of $x_t = 4\eta^2$. Our numerical results presented in §3 agree almost precisely with this formula.

Let us now see how these approximations allow us to balance the exact relations (1.7*a*) and (1.7*c*) almost precisely. To leading order, the mass in the shelf is given by

$$M_c(\tilde{t}) = \int_0^{\tilde{x}} q_c(x, \tilde{t})\, dx. \tag{2.7a}$$

By using (2.6) and the transformation $x = \int_0^t 4\eta^2\, dt$ on (2.7), we find

$$\begin{aligned} M_c(\tilde{t}) &= -4\eta_0 \exp\left(-\int_0^{\tilde{t}} \Gamma(s)\, ds\right)\left\{\int_0^{\tilde{t}} dt\, \frac{\Gamma(t)}{3} \exp\frac{1}{3}\int_0^t \Gamma(s)\, ds\right\} \\ &= 4\eta_0 \exp\left(-\int_0^{\tilde{t}} \Gamma(s)\, ds\right) - 4\eta_0 \exp\left(-\int_0^{\tilde{t}} \tfrac{2}{3}\Gamma(s)\, ds\right). \end{aligned} \tag{2.7b}$$

But the last term is simply $M_s(\tilde{t}) = \int_{-\infty}^{\infty} q_s(x, \tilde{t})\, dx$, the mass in the solitary wave, and thus to leading order

$$M(\tilde{t}) = M_c(\tilde{t}) + M_s(\tilde{t}) = 4\eta_0 \exp\left(-\int_0^{\tilde{t}} \Gamma(s)\, ds\right), \tag{2.8}$$

the exact result. A similar calculation can be carried out for $G(\tilde{t})$. When Γ is constant it can be done explicitly. We find, again to leading order, that

$$G(\tilde{t}) = (-16\eta_0^3/\Gamma) \exp(-\Gamma\tilde{t})\,[\exp(-\Gamma\tilde{t}) - 1], \tag{2.9}$$

which is the exact result (1.7*c*).

Finally we mention the consequences of these results in the context of shallow water waves. Integration of (2.1) gives

$$\eta/\eta_0 = (D_0/D)^{\frac{3}{2}}, \tag{2.10}$$

whence the soliton amplitude is

$$\tfrac{4}{3}\epsilon h \eta_0^2 D_0^3/D. \tag{2.11}$$

Thus the solitary wave amplitude is inversely proportional to the depth. On the other hand the shelf height (here it is convenient to express the height as a function of t, which in the water wave case measures position, and $\tilde{t}$ the present position of the solitary wave) is $\frac{2}{3}\epsilon h D^2(\tilde{t})\, q_c(x(t), \tilde{t})$, which, using (2.6) with $\Gamma = +9D_t/(4D)$, is

$$-3\epsilon h D' \frac{D^{\frac{9}{4}}(t)}{D_0^{\frac{3}{2}}} \frac{1}{D^{\frac{1}{4}}(\tilde{t})}, \tag{2.12}$$

which is inversely proportional to the fourth root of the depth estimated at the present solitary wave position. D' refers to the derivative of the depth with respect to the argument $\epsilon^{\frac{3}{2}}X/h$.

3. Numerical results

In order to verify the theoretical predictions, we numerically simulated the differential equation (1.1). For a number of reasons we chose an explicit finite-difference scheme suggested by Vliegenthart (1971). This scheme discretizes the components of (1.1) by

$$\left.\begin{aligned} q_t &= \frac{q(j,n+1)-q(j,n-1)}{2\Delta t}+O((\Delta t)^2),\\ q &= \frac{q(j+1,n)+q(j,n)+q(j-1,n)}{3}+O((\Delta x)^2),\\ q_x &= \frac{q(j+1,n)-q(j-1,n)}{2\Delta x}+O((\Delta x)^2),\\ q_{xxx} &= \frac{q(j+2,n)-2q(j+1,n)+2q(j-1,n)-q(j-2,n)}{2(\Delta x)^3}+O((\Delta x)^2), \end{aligned}\right\} \tag{3.1}$$

where $t = n\Delta t$ and $x = j\Delta x$.

We define $\Gamma(t) = -f_t(t)/f(t)$ and we will present the results of two numerical cases. Case (i) consists of defining $f(t) = e^{\sigma t}$ so that $\Gamma(t) = -\sigma =$ constant. For this case the computations used $\sigma = -\frac{1}{40}$ and considered times $0 < t < 100$. For case (ii) we took $f(t) = \sigma t - 1$, yielding $\Gamma(t) = -\sigma/(\sigma t - 1)$. In these computations we chose $\sigma = \frac{1}{40}$ and looked at times $0 < t < 40$. The choice of case (ii) is of interest because of its potential applicability as a model to the problem of an internal solitary wave travelling on a thermocline in the neighbourhood of the point where the coefficient of the nonlinear terms vanishes (approximately where the depths of the upper and lower layers are equal).

The time at which the perturbation procedure breaks down is when $\Gamma/3\eta$, the shelf height, is of the same order as the amplitude $2\eta^2$. For case (i) this occurs when t is $O(\ln|\sigma|/\sigma)$, which for $\sigma = -\frac{1}{40}$ is approximately 100 time units. We monitored times up to 100 time units for case (i) and did not observe any divergence between the numerical and perturbation results. For case (ii), the breakdown occurs when time is $\sigma^{-1} - O(\sigma^{-\frac{2}{3}})$, which for $\sigma = \frac{1}{40}$ is approximately 33 time units. After this time we noticed that the perturbation solution began to diverge from the numerical solution.

Figure 1 gives an overall picture of the total motion of the system. The major features of the solution are: (*a*) a slightly distorted solitary wave, (*b*) the formation of the shelf, its finite range and its subsequent evolution and (*c*) the decaying oscillatory tail. Figure 1 shows the numerical solution for all x at five different times t.

In order to check on the accuracy of the numerical results, we continuously monitored the values of the total mass, energy and the centre of gravity and compared the numerical results with the exact relations (1.7). First, with $\Gamma(t) = -f_t(t)/f(t)$ the mass is given by the relation

$$\int q\,dx = 4\eta_0|f|. \tag{3.2}$$

Second, the energy is given by

$$\int q^2\,dx = \tfrac{16}{3}\eta_0^3 f^2, \tag{3.3}$$

and, third, the centre of gravity is defined by

$$\bar{y} = \frac{\int xq\,dx}{\int q\,dx} = \frac{16\eta_0^3\{\int|f|\,dt\}}{4\eta_0|f|}. \tag{3.4}$$

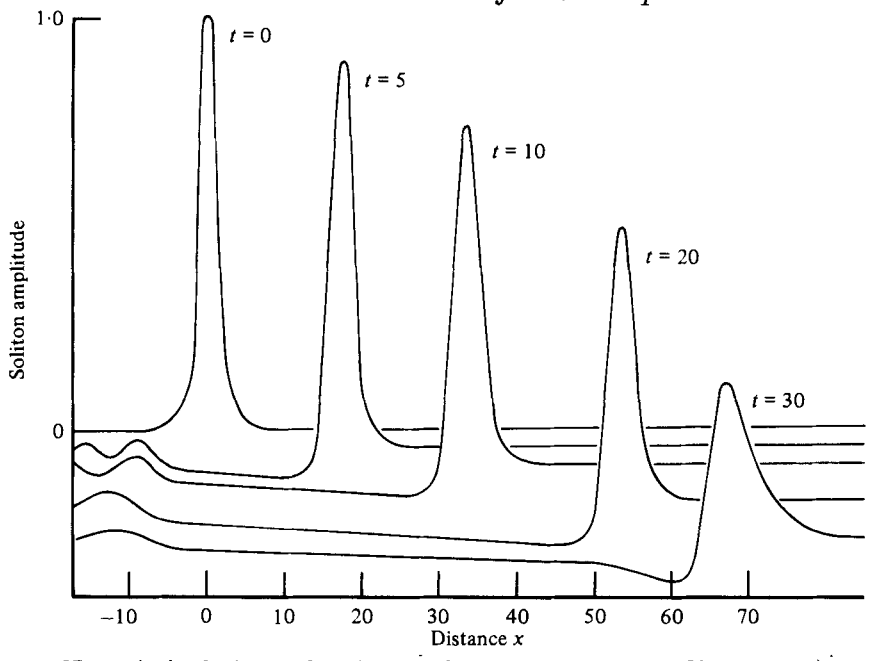

FIGURE 1. Numerical solution at five time levels $t = 0, 5, 10, 20, 30$. The curves shown graph the distance x $(-10 < x < 70)$ versus the scaled amplitude $(q(x, t)/2\eta_0^2)^{\frac{1}{2}}$.

	Case (i)	Case (ii)
Mass	0·0003 %	0·48 %
Energy	1·9 %	2·28 %
Centre of gravity	0·7 %	1·07 %

TABLE 1. The maximum error obtained in comparing the numerical results to the exact results, over the intervals (i) $0 < t < 100$ and (ii) $0 < t < 32$.

As the table 1 indicates, we obtained very close agreement with the exact results, which is to be anticipated since the Vliegenthart scheme is designed to conserve both mass and energy in the unperturbed equation.

Having established the accuracy of the numerical results, we now compare them with the results of the perturbation theory.

In analysing the solitary wave portion of the perturbation solution, two features were checked numerically, the amplitude and the position. The amplitude evolution as derived from the perturbation theory is given by

$$2\eta^2 = 2\eta_0^2 |f|^{\frac{1}{2}}. \tag{3.5}$$

Figure 2 gives a graphical representation of the comparison of the numerical results and (3.5) for case (i). The comparison shown in figure 2 yields a maximum error of 3 %.

The second feature of the solitary wave examined is its position, which, to leading order, is given by

$$\begin{aligned} x(\tilde{t}) &= \int_0^{\tilde{t}} 4\eta^2 \, dt + O(\Gamma) \\ &= 4\eta_0^2 \int_0^{\tilde{t}} |f|^{\frac{1}{2}} \, dt + O(\Gamma). \end{aligned} \tag{3.6}$$

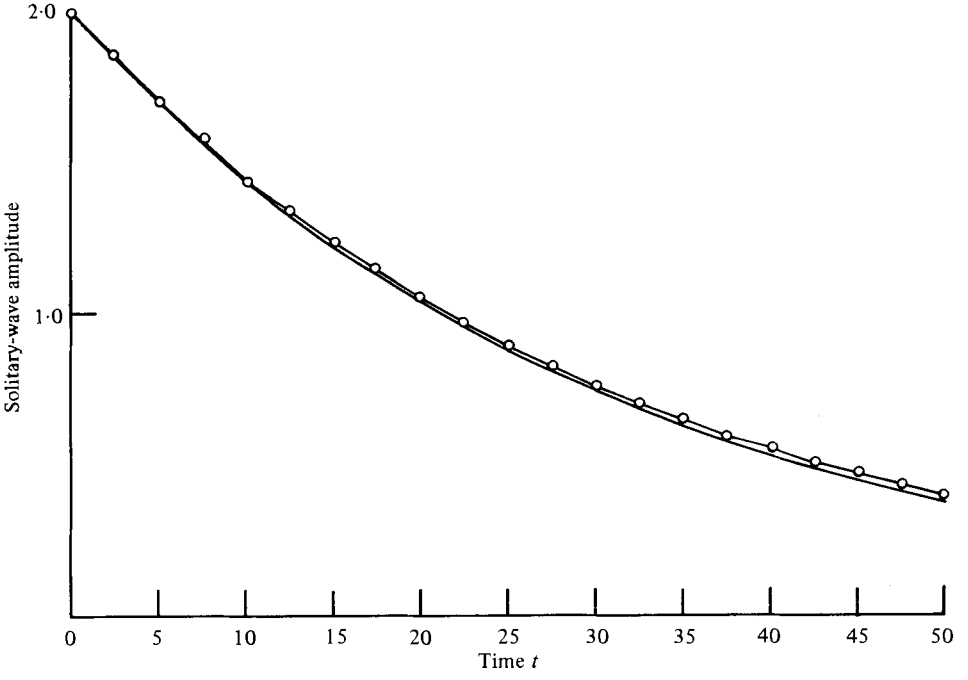

FIGURE 2. Numerical solution (—o—) versus perturbation theory (——) for the amplitude variation of the solitary wave. The results graph the amplitude ($0 < q(x, t) < 2$) versus time ($0 < t < 50$) for case (i).

The comparison between the integration of (3.6) and the numerical results for case (i) is given in figure 3.

Before we proceed there are two points to be made concerning the results shown in figure 3. First, from the numerical experiment, one observes that the solitary wave slows down and stops. Remarkably the integration of (3.6),

$$x(\tilde{t}) = (+3\eta_0^2/\Gamma)\,(1-\exp(-\tfrac{4}{3}\Gamma\tilde{t})),$$

follows the entire experimental trajectory of the solitary wave maximum to within 2 %, which is of order Γ. We say remarkably, for one might expect the approximate solution to be valid only for times when $t \ll \Gamma^{-1}\ln\Gamma^{-1}$ when $-\Gamma/3\eta$, the shelf height, is much less than $2\eta^2$, the soliton amplitude. Second, we note in figure 3 that the difference between theory and numerical experiment for the trajectory of the centre of gravity $\bar{y} = (4\eta_0^2/\Gamma)\,(1-\exp(-\Gamma\tilde{t}))$ is less than 0·7 %. In view of the fact that the approximate theory follows both $\int_{-\infty}^{\infty} q\,dx$ and $\int_{-\infty}^{\infty} xq\,dx$ so closely (cf. (2.8) and (2.9)), it is not surprising that $\bar{y}(t)$ can be followed so closely.

The comparison between the integration of (3.6) and the numerical results for case (ii) is given in figure 4. The maximum error for case (ii) was 2·3 %.

The second major feature of the general solution which we checked was the shelf and again the numerical and perturbation results were extremely close.

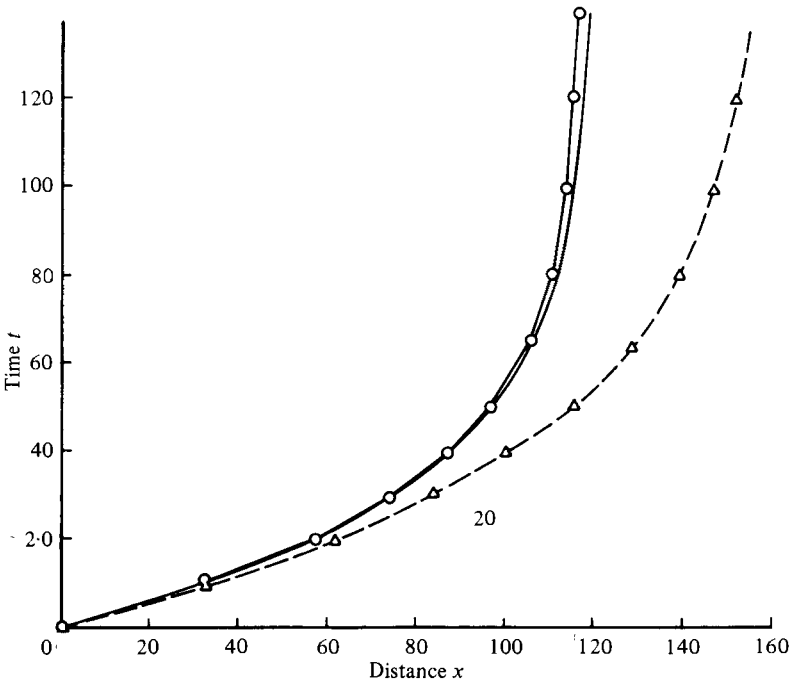

FIGURE 3. Numerical solution (—o—) versus perturbation theory (——) for the soliton position. Numerical solution (△) versus perturbation theory (– – –) for the centre of gravity. The results graph distance ($0 < x < 160$) versus time ($0 < t < 140$) for case (i).

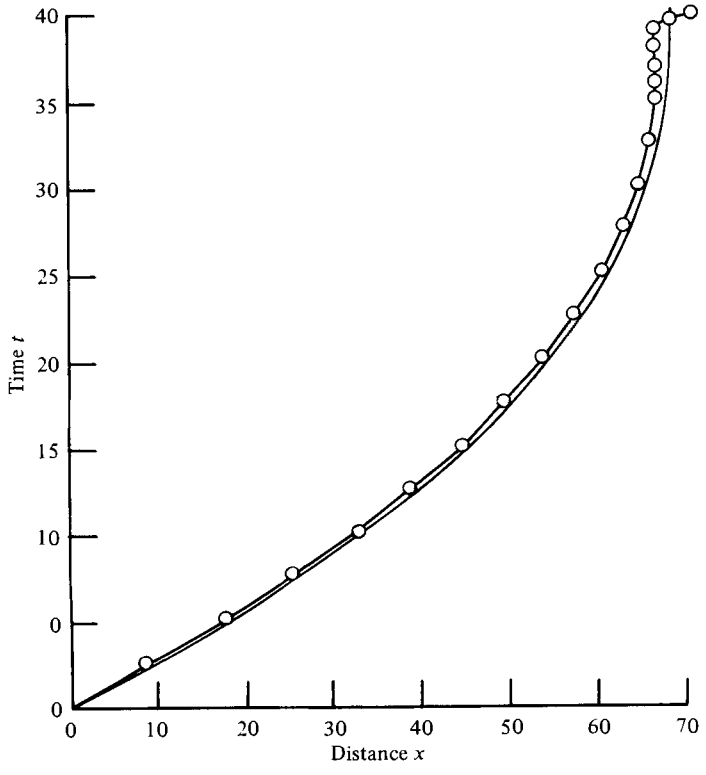

FIGURE 4. Numerical solution (—o—) versus perturbation theory (——) for soliton position. The results graph distance ($0 < x < 70$) versus time ($0 < t < 40$) for case (ii).

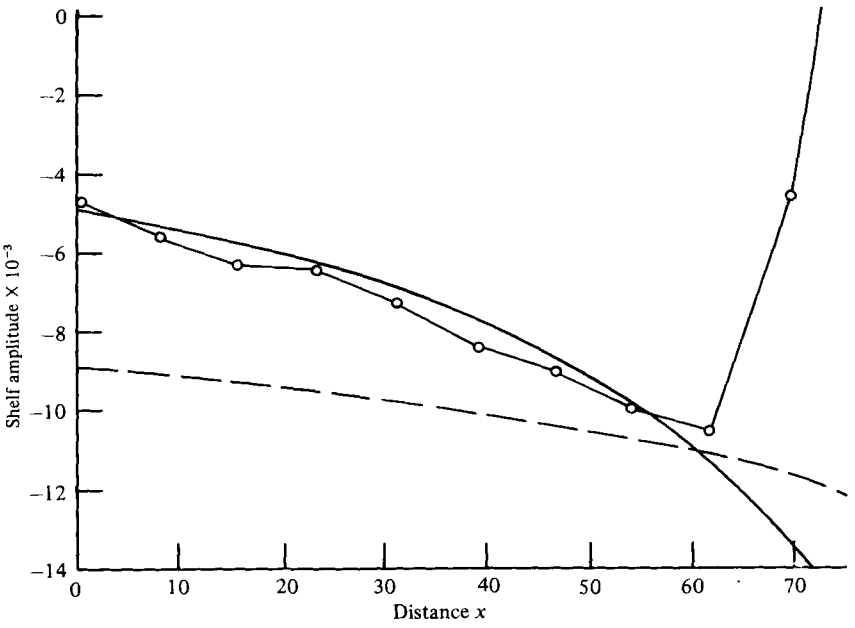

FIGURE 5. Numerical solution (—o—) versus perturbation theory (——) for shelf amplitude. The curves relate distance ($0 < x < 70$) and amplitude ($-14 \times 10^{-3} < q < 0$) for case (i) at $t = 27{\cdot}75$ time units. The dashed line (– – – –) represents the maximum amplitude of the shelf for each point x. This maximum occurs at $t = t_c(x)$ the creation time of the shelf at the point x. The rear portion of the solitary wave may be seen at the right of the figure.

From (2.6) with $\Gamma(t) = -f_t(t)/f(t)$, we find

$$q_c(x, \tilde{t}) = \frac{q_c(x, t_c(x))}{f(t_c(x))} f(\tilde{t}), \tag{3.7}$$

where $\tilde{t}$ measures the current time and $t_c(x)$ represents the time at which the shelf was created at each point x. By writing the creation time as a function of x through the integration of (3.6) we arrived at the following results. For case (i), (3.7) yields

$$q_c(x, \tilde{t}) = \frac{\sigma e^{\sigma \tilde{t}}}{3\eta_0 (1 + \sigma x/3\eta_0^2)^{\frac{5}{4}}}, \tag{3.8}$$

where $\eta_0 = \eta(t = 0)$.

Similarly for case (ii), it is easy to verify that

$$q_c(x, \tilde{t}) = \frac{\sigma(\sigma \tilde{t} - 1)}{3\eta_0 [1 - 7\sigma x/12\eta_0^2]^{\frac{8}{7}}}. \tag{3.9}$$

In figure 5 we look at an enlarged version of the solution for case (i) at $\tilde{t} = 27$ time units, and we focus our attention on the shelf portion of that solution. The dashed line just below the shelf represents the maximum amplitude of the shelf at each point x. This maximum, which is $-\Gamma(t_c)/3\eta(t_c)$, occurs at the time of its creation. The numerical results agree almost precisely with the perturbation results given by (3.8) and (3.9), and the comparison is equally good at all other times.

In order to study further the formation and evolution of the shelf, we focused our attention on several positions and monitored the evolution of the shelf at those points.

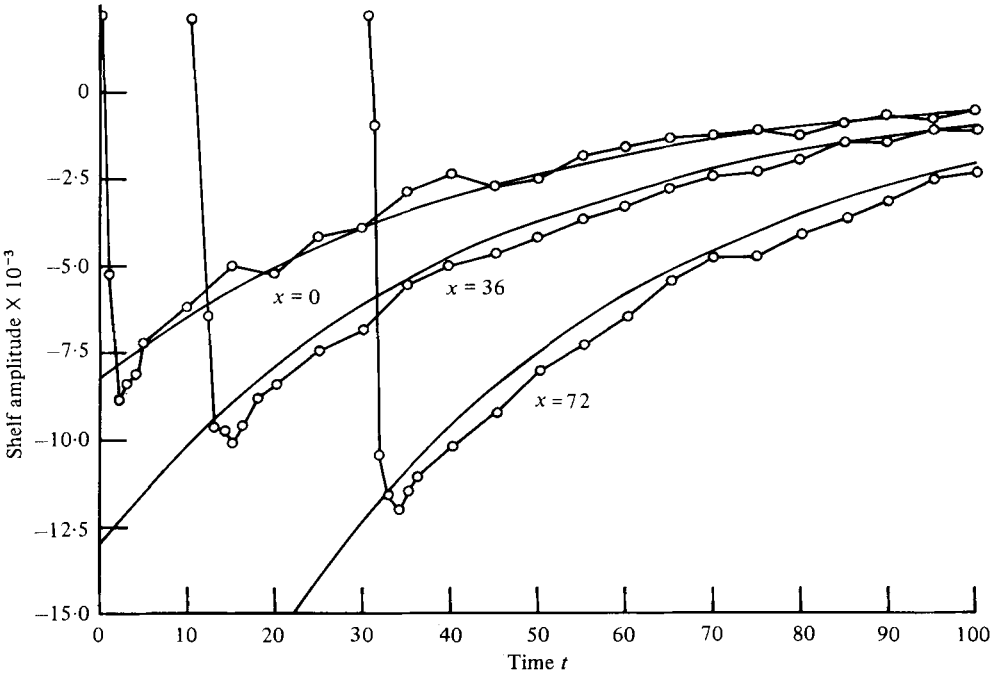

FIGURE 6. Numerical solution (—o—) versus perturbation theory (——) for shelf amplitude. The results which are quoted at $x = 0$ (initial soliton position), $x = 36$, and $x = 72$, graph shelf amplitude ($-15{\cdot}0 \times 10^{-3} < q(x, t) \leqslant 0$) versus time ($0 < t < 100$) for case (i). The rear portion of the solitary wave appears at the left of the figure.

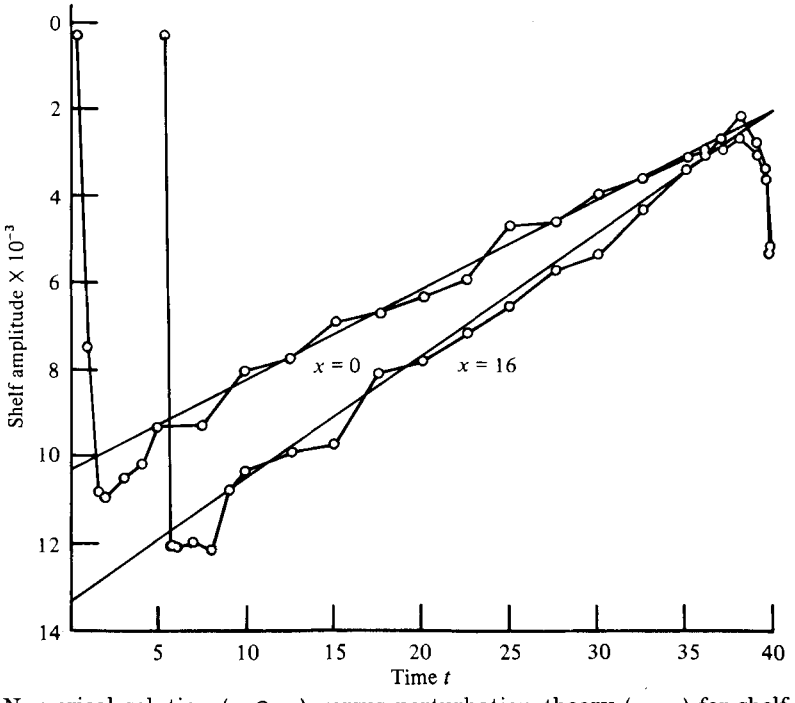

FIGURE 7. Numerical solution (—o—) versus perturbation theory (——) for shelf amplitude. The results which are quoted at $x = 0$ (initial soliton position) and $x = 16$ graph shelf amplitude ($-12{\cdot}0 \times 10^{-3} < q(x, t) < 2 \times 10^{-3}$) versus time ($0 < t < 40$) for case (ii). The rear portion of the solitary wave appears at the left of the figure.

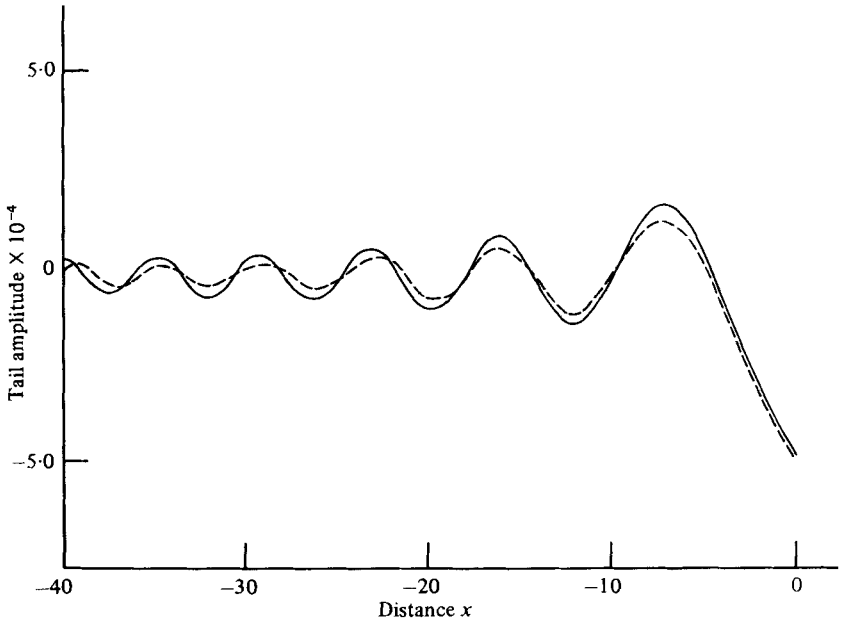

FIGURE 8. Numerical solution (—o—) versus perturbation theory (——) for oscillatory tail. The results graph tail amplitude ($-5{\cdot}0\times10^{-4} < q(x,t) < 5{\cdot}0\times10^{-4}$) *versus* distance ($-40 < x < 0$) for case (i) at $\tilde{t} = 7$ time units.

Figures 6 and 7 show in detail the evolution of the shelf after its initial formation and the perturbation and numerical results agree almost precisely. Although the slight differences between theory and experiment fall within the range of the numerical error, there is some suggestion of long waves propagating along the shelf from the solitary wave.

The results shown in figure 7 which are for case (ii) are qualitatively the same as case (i).

We also checked case (i) with $\sigma = +\frac{1}{40}$, the amplified case corresponding to an upward-facing shelf. After checking (3.8) against the numerical results we again found close agreement. Note that while the shelf amplitude decreases with x ($-\Gamma/3\eta(t_c)$ decreases with x), nevertheless at each point the shelf eventually grows with time (see (2.6), (3.8), with $\sigma = +\frac{1}{40}$). We remind the reader that the result (3.8) for the shelf is obtained by the balance $q_t = \sigma q$. Both qq_x and q_{xxx} are of smaller order. However, as the shelf grows, the nonlinear term again becomes important and indeed the shelf will begin to break and form order-one spatial derivatives on the time scale $\sigma^{-1}\ln\sigma^{-1}$. At this stage the dispersion becomes important; the shelf breaks into a solitary wave train, each pulse of which is weakly amplified by the σq term.

The last major portion of the solution considered was the oscillatory tail. This tail can be viewed in figure 1 for various time levels. In figure 8 we show a more detailed comparison of the perturbation results (2.3) and the numerical results for case (i) at $\tilde{t} = 7$ time units. The amplitude $\Gamma/3\eta$ in (2.3) has been adj usted to the value

$$(\Gamma(t_0)/3\eta(t_0))\exp\left(\int_{\tilde{t}}^{t_0}\Gamma(s)\,ds\right)$$

in line with (2.6) and (3.7); that is

$$q_{\text{tail}}(x,\tilde{t}) = \frac{\sigma e^{\sigma t}}{3\eta_0}\left[-\tfrac{2}{3} + \int_0^{x/(3\tilde{t})^{\frac{1}{3}}} \mathrm{Ai}\,(s)\,ds\right]. \tag{3.10}$$

The phase of the theoretical solution is not known exactly (the discrepancy is of the order of the width of the solitary wave) due to the lack of precise information as to where the shelf is formed with respect to the solitary wave. Therefore within this latitude we have chosen the phase of the theoretical solution (2.3) so that it agrees with the numerical solution at the point where the oscillatory tail attaches to the shelf. We believe that the slight remaining discrepancy between the theory and numerical experiment is due to the presence of very low-amplitude long waves which are continuously created at the solitary wave. As already noted some evidence for these waves is seen in figures 5–7. Indeed, a very careful examination of the time dependence in the oscillatory tail seems to indicate the presence of these long waves. However our present numerical scheme is not sufficiently accurate to study this very small effect in further detail.

The authors are grateful to NSF (MCS75-07548 A01) and ONR (N00014-76-C-0867) for support.

REFERENCES

DJORDJEVIC, V. D. & REDEKOPP, L. G. 1978 The fission and disintegration of internal solitary waves moving over two-dimensional topography. *J. Phys. Oceanog.* **8**, 1016–1024.

FLASCHKA, H. & NEWELL, A. C. 1975 *Dynamical Systems, Theory and Applications* (ed. J. Moser), Lecture Notes in Physics, vol. 38, p. 335. Springer.

GARDNER, C. S. 1971 The Korteweg–de Vries equation as a Hamiltonian system. *J. Math. Phys.* **12**, 1548–1551.

GARDNER, C. S., GREENE, J. M., KRUSKAL, M. D. & MIURA, R. M. 1967 Method for solving the Korteweg deVries equation. *Phys. Rev. Lett.* **19**, 1095–1097.

GARDNER, C. S., GREENE, J. M., KRUSKAL, M. D. & MIURA, R. M. 1974 Korteweg–de Vries equation and generalizations. VI. Methods for exact solution. *Comm. Pure Appl. Math.* **27**, 97–133.

GRIMSHAW, R. 1970 The solitary wave in water of variable depth. *J. Fluid Mech.* **42**, 639–656.

GRIMSHAW, R. 1971 The solitary wave in water of variable depth. Part 2. *J. Fluid Mech.* **46**, 611–622.

JOHNSON, R. S. 1973*a* Asymptotic solution of the Korteweg–de Vries with slowly varying coefficients. *J. Fluid Mech.* **60**, 813–824.

JOHNSON, R. S. 1973*b* On the development of a solitary wave moving over an uneven bottom. *Proc. Camb. Phil. Soc.* **73**, 183–203.

KAKUTANI, T. 1971 Effects of an uneven bottom on gravity waves. *J. Phys. Soc. Japan* **30**, 272–276.

KARPMAN, V. I. & MASLOV, E. M. 1977 A perturbation theory for the Korteweg–de Vries equation. *Phys. Lett.* A **60**, 307–308.

KAUP, D. J. & NEWELL, A. C. 1978 Solitons as particles and oscillators and in slowly varying media: a singular perturbation theory. *Proc. Roy. Soc.* A **361**, 413–446.

KO, K. & KUEHL, H. H. 1978 Korteweg–de Vries soliton in a slowly varying medium. *Phys. Rev. Lett.* **4**, 233–236.

LEIBOVICH, S. & RANDALL, J. D. 1971 Dissipative effects on nonlinear waves in rotating fluids. *Phys. Fluids* **14**, 2559–2561.

LEIBOVICH, S. & RANDALL, J. D. 1973 Amplification and decay of long nonlinear waves. *J. Fluid Mech.* **58**, 481–493.

MILES, J. W. 1979 On the Korteweg–de Vries equation for a gradually varying channel. *J. Fluid Mech.* **91**, 181–190.

NEWELL, A. C. 1978 Soliton perturbation and nonlinear focussing, symposium on nonlinear structure and dynamics in condensed matter. In *Solid State Physics*, vol. 8, pp. 52–68. Oxford University Press.

NEWELL, A. C. 1980 The inverse scattering transform. *Solitons* (ed. R. K. Bullough) *Topics in Current Physics*, vol. 17, Springer.

OTT, E. & SUDAN, R. N. 1970 Damping of solitary waves. *Phys. Fluids* **13**, 1432–1434.

PEREGRINE, D. H. 1967 Long waves on a beach. *J. Fluid Mech.* **27**, 815–827.

TAPPERT, F. & ZABUSKY, N. J. 1971 Gradient-induced fission of solitons. *Phys. Rev. Lett.* **27**, 1774–1776.

VLIEGENTHART, A. C. 1971 On finite difference methods for the Korteweg–de Vries equation. *J. Engng Math.* **5**, 137–155.

ZABUSKY, N. J. & KRUSKAL, M. D. 1965 Interactions of solitons in a collisionless plasma and the recurrence of initial states. *Phys. Rev. Lett.* **15**, 240–243.

ZAKHAROV, V. E. & FADDEEV, L. D. 1971 The Korteweg–de Vries equation. A completely integrable Hamiltonian system. *Anal. Priloz.* **5**, 18.